Synthesis, Properties and Crystal Structures of $[Mo^{V}L(O)I_2]PF_6$, $[Mo^{IV}L(O)I_2]$, $[Mo^{V}L(O)(OMe)_2]PF_6$, $[Mo^{VI}LO_2(OMe)]BPh_4$ and $[Mo_2L_2O_3(\mu\text{-}O)I][BPh_4]_2$ (L = 1,4,7-trimethyl-1,4,7-triazacyclononane)†

Kai Silke Bürger,[a] Gabriele Haselhorst,[a] Stefan Stötzel,[a] Thomas Weyhermüller,[a] Karl Wieghardt*,[a] and Bernhard Nuber[b]

[a] *Lehrstuhl für Anorganische Chemie I, Ruhr-Universität, D-4630 Bochum, Germany*

[b] *Anorganisch-Chemisches Institut der Universität, D-6900 Heidelberg, Germany*

A series of mononuclear oxomolybdenum-(IV), -(V) and -(VI) complexes has been prepared from the precursor complex $[Mo^{V}L(O)I_2]PF_6$ **2** where L = 1,4,7-trimethyl-1,4,7-triazacyclononane. Compound **2** is reduced by NEt_3 in MeCN yielding $[Mo^{IV}L(O)I_2]$ **3**. The iodide ligands in **2** may be substituted by alkoxy ligands generating paramagnetic mononuclear complexes $[Mo^{V}L(O)(OMe)I]PF_6$ **4** and $[Mo^{V}L(O)(OMe)_2]PF_6$ **5**. The latter is oxidized by H_2O_2 to $[Mo^{VI}LO_2(OMe)]BPh_4$ **6**. Complex **2** was found to form the dinuclear diamagnetic species $[Mo^{V}_2L_2O_2(\mu\text{-}O)I_2][PF_6]_2$ **7** which generates the asymmetric, diamagnetic mixed-valence complex $[I(O)LMo^{IV}(\mu\text{-}O)Mo^{VI}LO_2]BPh_4$ **8** in the presence of NaOH. Complex **8** undergoes a reversible one-electron-transfer oxidation and paramagnetic $[I(O)LMo^{V}(\mu\text{-}O)Mo^{VI}LO_2][BPh_4]_2$ **9** has been isolated. The electrochemical, magnetic, and electronic structural as well as infrared and ESR spectral properties of the new complexes have been investigated. The structures of **2**, **3**, **5**, **6** and **9** have been determined by X-ray crystallography.

The co-ordination chemistry of mononuclear oxomolybdenum-(IV), -(V) and -(VI) complexes has in the past decade received a great deal of attention[1] owing to their biological relevance for oxotransferases.[2] The interconversion of monooxo, *cis*-dioxo and *cis*-trioxo octahedral molybdenum species (Scheme 1) with increasing formal oxidation states of the molybdenum ion is well established. The most intensively studied class of compounds contains facially co-ordinated chelating tridentate N-donor ligands: 1,4,7-triazacyclononane[3-7] (and derivatives thereof) or the anion hydrotris(pyrazolyl)borate(1−).[8-17] Their structural, magnetic and electronic properties have been studied by X-ray diffraction, ESR, infrared and resonance-Raman[15] spectroscopy. Mononuclear species are synthetically often difficult to obtain due to the thermodynamic stability and inertness of oxo-bridges. Thus corner- and edge-sharing, octahedral dinuclear species constitute a large class of compounds.[1,2c] In recent years a few mixed-valence oxo-bridged dinuclear species have been characterized and their electronic structures elucidated.[18-21] Localized[19-21] and delocalized[5,18] valences (class I or III according to the Robin and Day[22] classification scheme) have been described.

Here we describe some synthetic chemistry which yields mono- and di-nuclear species in a great variety. We have found that the oxidation product of $[Mo^{III}LI_3]$ **1**[4] in nitric acid, *i.e.* the monomeric complex $[Mo^{V}L(O)I_2]^+$ **2** (L = 1,4,7-trimethyl-1,4,7-triazacyclononane), is a very useful starting material for the synthesis of both mono- and di-nuclear complexes because the iodo ligands are labile and are readily substituted by a variety of ligands contrasting in this respect the chloro and bromo analogues which are quite robust.[4] Scheme 2 summarizes the preparative routes employed for mononuclear species whereas Scheme 3 shows the new dinuclear species prepared. Since much of this chemistry has been developed for the [hydrotris(pyrazolyl)borato]molybdenum complexes we are able to assess the generality of some structure–reactivity relationships discovered for this class of compounds.

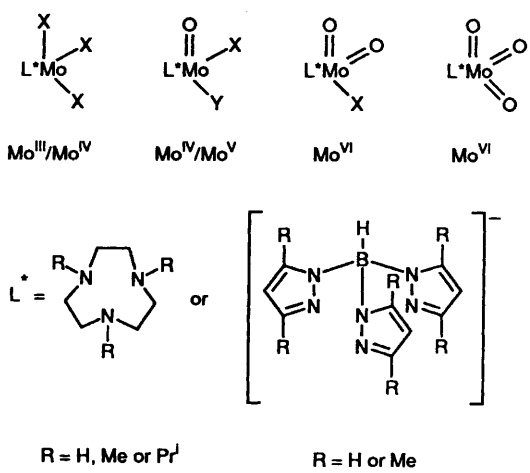

Scheme 1

Results

Syntheses and Spectroscopic Characterization of Complexes.—Table 1 gives infrared data whereas Table 2 summarizes electronic spectra and magnetic data for the complexes.

The most important starting material for the synthesis of mono- and di-nuclear oxomolybdenum complexes described in this work is $[Mo^{V}L(O)I_2]PF_6$ **2** which is readily available in good yields from the reaction of $[Mo^{III}LI_3]$ **1** with concentrated nitric acid.[4] The solution fluorescence and photoredox behaviour of **2** has recently been described.[23] Dark green crystals of **2** are soluble in water and common organic solvents *e.g.*

† *Supplementary data available:* see Instructions for Authors, *J. Chem. Soc., Dalton Trans.*, 1993, Issue 1, pp. xxiii–xxviii.

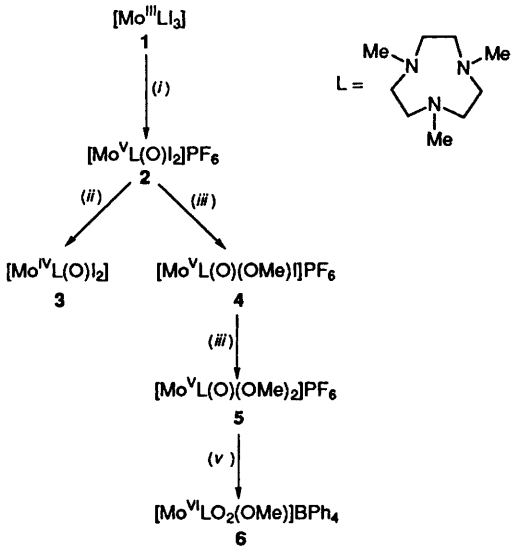

Scheme 2 Synthesis of mononuclear complexes. (*i*) 7 mol dm^{-3} HNO_3; (*ii*) MeCN,NEt_3; (*iii*) MeOH–Tl(OMe); (*iv*) MeOH–H_2O_2

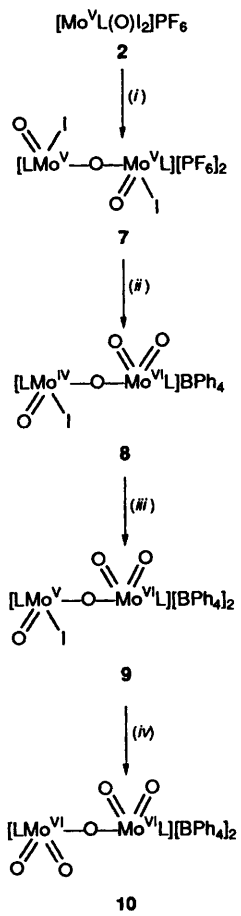

Scheme 3 Synthesis of dinuclear complexes. (*i*) Tl(acac),MeCN; (*ii*) NaOH,$NaBPh_4$; (*iii*) MeCN,$[Fe(C_5H_5)_2]PF_6$; (*iv*) MeCN–water–O_2

acetonotrile. In the infrared (KBr disc) the ν(Mo=O) stretching frequency is observed at 976 cm^{-1}; a temperature-independent (80–298 K) magnetic moment of 1.73 is characteristic of mononuclear Mo^V (d^1). Fig. 1 shows the X-band ESR spectra of solid samples of **2** and **5** (see below) at 10 K. Complex **2** displays a slightly anisotropic signal at $g_{av} \approx 2.03$. The electronic spectrum of **2** in MeCN exhibits two fairly intense (d–d) absorption maxima at 661 and 470 nm (Table 2) which may be assigned to $^2B_2 \longrightarrow {}^2E$ and $^2B_2 \longrightarrow {}^2B_1$ transitions in D_{4h}

Table 1 The ν(Mo=O) and ν(Mo–O–Mo) stretching bonds (cm^{-1}) of the complexes

Complex	ν(Mo=O)	ν(Mo–O–Mo)
2	976	
3	958	
4	958	
5	934	
6	928, 906	
7	962	749
8	960, 905, 870	*b*
9	964, 931, 905	*b*
10[a]	942, 917	*b*

[a] $[Mo^{VI}_2L_2O_5][BPh_4]_2$. [b] Not detected due to strong bands of the $[BPh_4]^-$ anion.

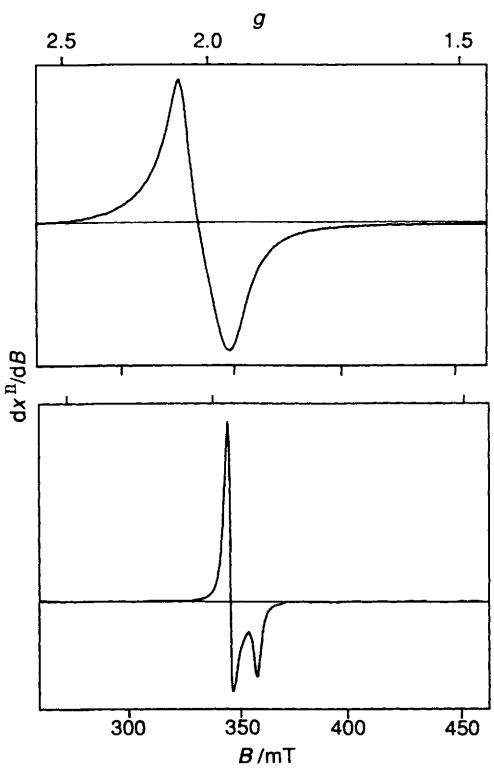

Fig. 1 X-Band ESR spectra of solid samples of $[Mo^VL(O)I_2]PF_6$ **2** (top) and $[Mo^VL(O)(OMe)_2]PF_6$ **5** (bottom) at 10 K (9.43 GHz)

symmetry although their intensities seem to indicate some ligand-to-metal charge-transfer character.

When a deoxygenated solution of complex **2** in MeCN was treated with triethylamine pink crystals of $[Mo^{IV}L(O)I_2]$ **3** precipitated in 84% yield. Complex **3** is the one-electron reduction product of **2**. In the infrared spectrum the ν(Mo=O) stretching frequency is shifted to 958 cm^{-1}. Compound **3** is diamagnetic (d^2). Fig. 2 shows the electronic spectra of **2** and **3**. Note the very different intensities of the absorption maxima of the two species (Table 2, Fig. 2).

Both iodo ligands in complex **2** may be sequentially substituted by alkoxyl groups in the presence of $Tl^I(OR)$ salts which facilitate this substitution by removal of the iodide ions as insoluble TlI. Thus the reaction of **2** in deoxygenated methanol with 1 or 2 equivalents of $Tl^I(OMe)$ leads to the formation of dark green $[MoL(O)(OMe)I]PF_6$ **4** and blue $[MoL(O)(OMe)_2]PF_6$ **5**, respectively. Complex **4** was always found to be contaminated with starting material **2** and the bis(methoxo) complex **5** in various amounts. We therefore did not characterize this species fully. Substitution of the two iodo ligands in **2** by strong π-donor methoxo ligands in **5** brings about a

Table 2 Electronic spectral data and magnetic properties of the complexes

Complex	λ_{max}/nm (ε/dm^3 mol^{-1} cm^{-1})[a]	μ_{eff}(298 K)
1	1085 (7), 721 (46), 469 (sh), 374 (5500), 332 (2450), 304 (3500)	3.63
2	661 (1850), 470 (915), 360 (3300)	1.73
3	829 (60), 700 (sh), 530 (46)	*b*
5	700 (25), 232 (5200)	1.71
6	*c*	*b*
7	713 (670), 495 (9500), 402 (2900), 241 (15 000)	*b*
8	943 (600), 570 (3000), 473 (2500)	*b*
9	890 (124), 480 (sh), 420 (2300), 320 (sh)	1.78
10	*c*	*b*

[a] Measured in MeCN. [b] Diamagnetic. [c] Colourless.

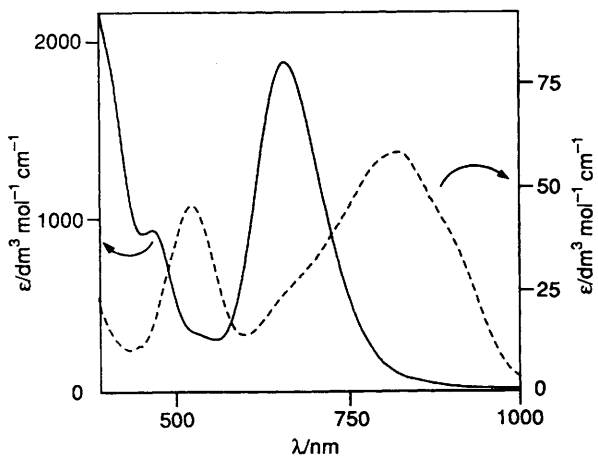

Fig. 2 Electronic spectra of $[Mo^{V}L(O)I_2]PF_6$ **2** (——) and $[Mo^{IV}L(O)I_2]$ **3** (– – –) in MeCN

weakening of the Mo^{V}=O bond. Thus the ν(Mo=O) stretching frequency is observed at 934 cm^{-1} whereas for **4** this vibration is detected at 958 cm^{-1} (Table 1). The temperature-independent magnetic moment of 1.71 is again indicative of a molybdenum(V) (d^1) electronic configuration. The X-band ESR spectrum (Fig. 1) of solid **5** at 10 K shows an axial spectrum with g values at 1.95 and 1.88 (g_{iso} = 1.93).

Oxidation of a blue solution of complex **5** in methanol with H_2O_2 yielded a colourless solution from which upon addition of $NaPF_6$ colourless crystals of $[Mo^{VI}LO_2(OMe)]PF_6$ **6** precipitated. Complex **6** contains a *cis*-dioxomolybdenum(VI) moiety as is clearly seen in the infrared spectrum where two ν(Mo=O) stretching modes (ν_{sym} and ν_{asym}) are observed at 928 and 906 cm^{-1}. Complex **6** is diamagnetic (d^0).

In the following we will discuss the preparation of dinuclear species (Scheme 2). When to an MeCN solution of complex **2** (containing ≈2% water) was added an equimolar amount of Tl^{I}(acac) [acac = pentane-2,4-dionate(1−)] and the mixture was heated under an argon atmosphere to reflux a change from dark green to red-brown was observed. From this solution red-brown microcrystals of $[Mo^{V}_2L_2O_2(\mu\text{-}O)I_2][PF_6]_2$ **7** were obtained in 52% yield. Complex **7** is diamagnetic. In the infrared spectrum bands at 962 and 749 cm^{-1} indicate the presence of a terminal Mo=O and a bridging Mo–O–Mo moiety, respectively.

$$2[Mo^{V}L(O)I_2]^+ + 2Tl(acac) + H_2O \longrightarrow [Mo^{V}_2L_2(O)_2(\mu\text{-}O)I_2]^{2+} + 2TlI + 2Hacac \quad (1)$$

In principle, two geometric isomers of **7** exist. Assuming a linear Mo–O–Mo unit in both forms an isomer **A** of C_2 symmetry (C_2 axis through the μ-oxo atom with respect to the iodo ligands) or an isomer **B** of C_i symmetry may be found. Lacking crystal structures we have not been able to discern

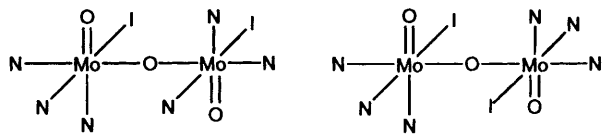

between these two possibilities but it is noted that both isomers have been crystallographically characterized for the tris(pyrazolyl)borato analogue $[\{Mo^{V}[HB(pz)_3](O)Cl\}_2O]$.[19] The electronic spectra of these two isomers and of **7** (Fig. 3) display a very intense ($\varepsilon > 9.0 \times 10^3$ dm^3 mol^{-1} cm^{-1}) absorption maximum in the visible which Lincoln and Loehr[15] have recently identified by resonance-Raman excitation profiles as a charge-transfer transition of the $[Mo^{V}_2O_2(\mu\text{-}O)]^{4+}$ moiety. A similar absorption maximum has been reported for $[Mo^{V}_2O_2(\mu\text{-}O)Br_4(bipy)_2]$ (bipy = 2,2′-bipyridine) at 510 nm[24] and at ≈450 nm for the dinuclear species $[Mo^{V}_2O_2(\mu\text{-}O)Cl_8]^{4-}$ formed in 5–6 mol dm^{-3} HCl which also contains the linear $[Mo_2O_2(\mu\text{-}O)]^{4+}$ unit.[15,25] Thus the observed vibrational and electronic spectra together with its diamagnetism support the assignment of structure **A** or **B** to complex **7**; a linear (or nearly linear) $[Mo^{V}_2O_2(\mu\text{-}O)]^{4+}$ unit is clearly present. It is noted that the ν(Mo=O) stretching mode in **7** is shifted by 14 cm^{-1} to lower wavenumbers as compared to its mononuclear precursor $[Mo^{V}L(O)I_2]^+$ **2**. This effect is probably an indicator for the stronger π-donor ability of a μ-oxo bridge in **7** as compared to an iodo ligand in **2** which weakens the terminal Mo=O bond.

When to a red-brown solution of complex **7** in acetone or MeCN was added a solution of aqueous NaOH in the presence or absence of oxygen the colour changed within a few minutes to blue-violet. Addition of $NaBPh_4$ to this solution initiated the precipitation of deep blue microcrystals of *diamagnetic* $[Mo_2L_2O_3(\mu\text{-}O)I]BPh_4$ **8**. The infrared spectrum proved to be quite informative in the ν(Mo=O) region (800–1000 cm^{-1}). Three ν(Mo=O) stretching vibrations at 870, 905 and 960 cm^{-1} are observed. Comparison of these data with those of the mononuclear complexes **3** and **6** (Table 1) allows the conclusion that **8** contains a $[Mo^{IV}L(O)(\mu\text{-}O)I]^-$ unit with one terminal Mo=O group and a $[Mo^{VI}LO_2(\mu\text{-}O)]$ moiety with a *cis*-dioxomolybdenum(VI) fragment. Thus the monocation in crystals of **8** is an asymmetric $Mo^{IV}Mo^{VI}$ mixed-valence species. In principle, the formulation as a Mo^{V}_2 dinuclear complex with intramolecularly antiferromagnetically coupled d^1d^1 centres is also conceivable. On the other hand, it is well established that octahedral molybdenum(V) complexes containing a *cis*-dioxo unit are extremely strong reductants and have, in fact, not been characterized to date whereas oxomolybdenum(IV) and *cis*-dioxomolybdenum(VI) species are well known. It is interesting in this context that Young *et al.*[21] recently reported the crystal structure of a similar mixed-valence $W^{IV}W^{VI}$ complex $[\{HB(pz)_3\}O_2W^{VI}(\mu\text{-}O)W^{IV}O(CO)\{HB(pz)_3\}]$. Therefore, we propose the structure shown for **8**. The electronic spectrum in MeCN is shown in Fig. 3 (Table 2).

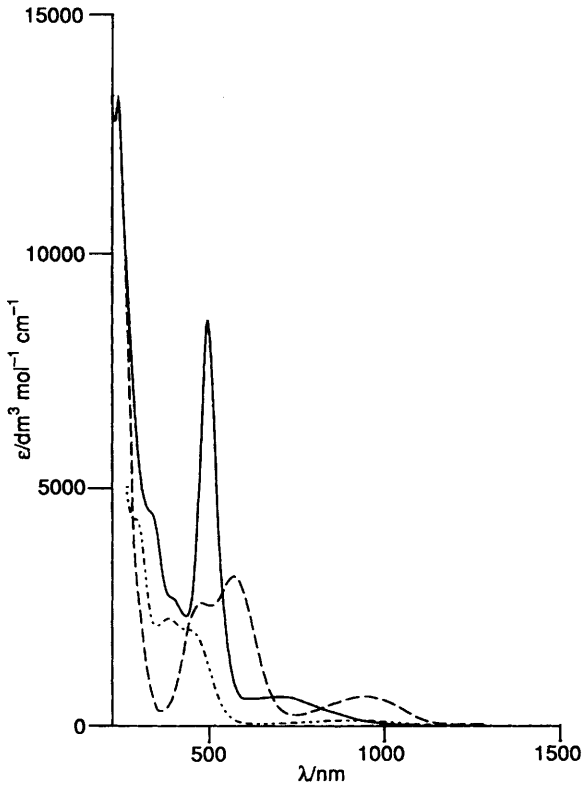

Fig. 3 Electronic spectra of dinuclear complexes **7** (——), **8** (– – –) and **9** (· · ·) in MeCN

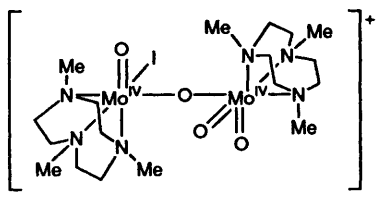

8

The formation of complex **8** from **7** may be rationalized as follows. The nucleophile OH^- replaces I^- in **7** forming the dinuclear $[Mo^V_2L_2(O_2)(\mu\text{-}O)(OH)I]^{2+}$ intermediate which upon deprotonation of the co-ordinated hydroxo group undergoes a rapid intramolecular electron-transfer reaction with formation of the asymmetric $Mo^{IV}Mo^{VI}$ species **8**. Interestingly, **8** may be oxidized electrochemically (see below) or chemically by one electron. Dropwise addition of a MeCN solution of ferrocenium hexafluorophosphate to a solution of **8** in MeCN (1:2) results in a change from deep blue to red-orange. Upon addition of $Na[BPh_4]$ orange microcrystals of $[Mo_2L_2(O)_3(\mu\text{-}O)I][BPh_4]_2$ **9** precipitated. Complex **9** is paramagnetic; a temperature-independent magnetic moment of 1.78 per dinuclear unit (80–298 K) has been calculated. In the X-band ESR spectrum of solid **9** a nearly isotropic signal is observed at $g = 1.97$. In the infrared spectrum three ν(Mo=O) bands at 964, 931 and 905 cm^{-1} indicate the presence of a $[Mo^VL(O)(\mu\text{-}O)I]$ and a $[Mo^{VI}LO_2(\mu\text{-}O)]$ fragment. Complex **9** is therefore the one-electron oxidation product of **8** where the molybdenum(IV) ion has been oxidized to Mo^V. The electronic spectrum is shown in Fig. 3; it is very similar to that of the recently characterized species $[Mo_2\{HB(pz)_3\}_2O_4Cl]$[20] which is the tris(pyrazolyl)borate analogue of **9**.

Finally, the asymmetric mixed-valence species **9** is slowly oxidized by air in MeCN solution which contains ≈2% of water with formation of the colourless, symmetric complex $[Mo^{VI}_2L_2O_4(\mu\text{-}O)][BPh_4]_2$ **10**. In the infrared spectrum only two ν(Mo=O) stretching frequencies at 942 and 917 cm^{-1} are observed. This diamagnetic compound has been previously described and structurally characterized.[5]

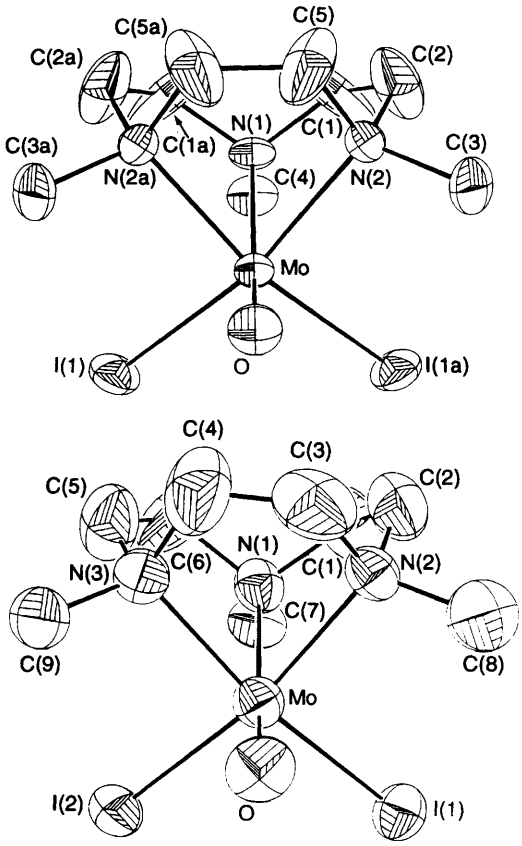

Fig. 4 Structures of the monocation in crystals of complex **2** (top) and of the neutral molecule in crystals of **3** (bottom)

Description of Crystal Structures.—Fig. 4 (top) shows the structure of the monocation $[Mo^VL(O)I_2]^+$ in crystals of **2**; Table 3 summarizes important bond lengths and angles. Crystals of **2** consist of pseudo-octahedral cations $[Mo^VL(O)I_2]^+$ and PF_6^- anions. The cation possesses crystallographically imposed site symmetry *m* [atoms Mo(1), O(1), N(1) and C(4) lie on a mirror plane] which is not compatible with the (λλλ) or (δδδ) conformation of the three five-membered chelate rings Mo–N–C–C–N of the co-ordinated cyclic triamine. Consequently, the methylene carbon atoms display physically meaningless large anisotropic thermal parameters which lead to unrealistically short C–C bond distances. Attempts to model this disorder by a split-atom model failed. This problem has been encountered in many crystal structure determinations of complexes containing an ML fragment[3] and will not be discussed further here.

The structure of the neutral molecule $[Mo^{IV}L(O)I_2]$ in crystals of **3** is shown in Fig. 4 (bottom). The overall geometry of this oxomolybdenum(IV) complex is completely analogous to that of the monocation in **2**. In this instance the molecule does not possess crystallographically imposed symmetry. The Mo^{IV} in **3** or Mo^V in **2** is in a pseudo-octahedral environment of a tridentate, facially co-ordinated triamine L, a terminal oxo and two iodide ligands in *cis* position with respect to each other. The Mo=O bond lengths in both structures are identical within experimental error (average 1.67 Å) and indicate a double (or even triple) bond.[26] The Mo=O bond exerts a pronounced structural *trans* influence on the Mo–N bond in *trans* position. Thus the difference of the $Mo–N_{trans}$ and the average $Mo–N_{cis}$ bond lengths in the two structures are 0.12 Å for **2** and 0.13 Å

Table 3 Selected bond distances (Å) and angles (°) of complexes

Complex **2**				Complex **5**			
Mo–I(1)	2.693(1)	Mo–O	1.666(8)	Mo–N(1)	2.352(9)	Mo–O(2)	1.918(7)
Mo–N(1)	2.368(9)	Mo–N(2)	2.250(7)	Mo–N(2)	2.285(7)	Mo–O(1)	1.681(9)
				O(2)–C(6)	1.432(13)		
I(1)–Mo–O	101.4(2)	O–Mo–N(1)	160.5(3)	N(1)–Mo–O(1)	159.2(4)	N(1)–Mo–O(2)	87.2(2)
I(1)–Mo–N(1)	92.1(1)	O–Mo–N(2)	90.5(3)	O(1)–Mo–O(2)	106.0(3)	O(2)–Mo–O(2A)	98.8(4)
I(1)–Mo–N(2)	165.7(2)	N(1)–Mo–N(2)	74.5(2)	O(1)–Mo–N(2)	89.1(3)	O(2)–Mo–N(2)	88.7(3)
I(1)–Mo–I(1A)	91.6(1)	N(2)–Mo–N(2A)	77.8(3)	N(2)–Mo–N(2A)	78.8(4)	N(1)–Mo–N(2)	75.0(2)
I(1)–Mo–N(2A)	93.9(2)			Mo–O(2)–C(6)	135.3(6)		
Complex **3**				Complex **6**			
Mo–I(1)	2.789(2)	Mo–N(1)	2.375(18)	Mo–N(1)	2.258(3)	Mo–O(2)	1.792(4)
Mo–I(2)	2.794(2)	Mo–N(2)	2.254(16)	Mo–N(2)	2.318(4)	Mo–O(3)	1.783(4)
Mo–O	1.672(12)	Mo–N(3)	2.229(16)	Mo–N(3)	2.306(4)	Mo–O(1)	1.895(3)
				O(1)–C(10)	1.391(9)		
I(1)–Mo–I(2)	87.9(1)	I(2)–Mo–O	101.1(5)	N(1)–Mo–O(2)	91.6(1)	N(1)–Mo–N(2)	76.6(1)
I(1)–Mo–O	99.6(5)	I(2)–Mo–N(1)	90.8(4)	O(2)–Mo–N(2)	86.4(1)	N(1)–Mo–O(3)	87.5(1)
I(1)–Mo–N(1)	90.6(4)	I(2)–Mo–N(2)	166.4(4)	O(2)–Mo–O(3)	105.9(2)	N(2)–Mo–O(3)	160.3(1)
I(1)–Mo–N(2)	96.0(4)	I(2)–Mo–N(3)	94.7(4)	N(1)–Mo–N(3)	76.4(1)	O(2)–Mo–N(3)	159.7(2)
I(1)–Mo–N(3)	166.9(4)	O–Mo–N(1)	164.5(6)	N(2)–Mo–N(3)	75.0(1)	O(3)–Mo–N(3)	90.1(2)
N(1)–Mo–N(2)	76.2(6)	O–Mo–N(2)	91.2(6)	N(1)–Mo–O(1)	159.7(1)	O(2)–Mo–O(1)	102.2(2)
N(1)–Mo–N(3)	76.5(6)	O–Mo–N(3)	92.5(6)	N(2)–Mo–O(1)	89.4(1)	O(3)–Mo–O(1)	102.6(2)
N(2)–Mo–N(3)	78.8(6)			N(3)–Mo–O(1)	85.9(1)	Mo–O(1)–C(10)	135.4(4)

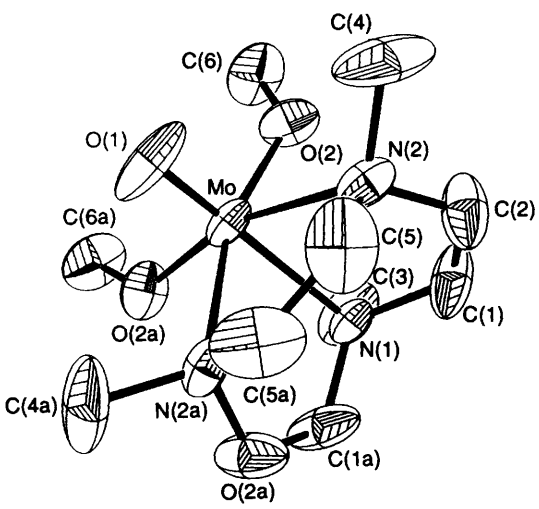

Fig. 5 Structure of the monocation in crystals of complex **5**

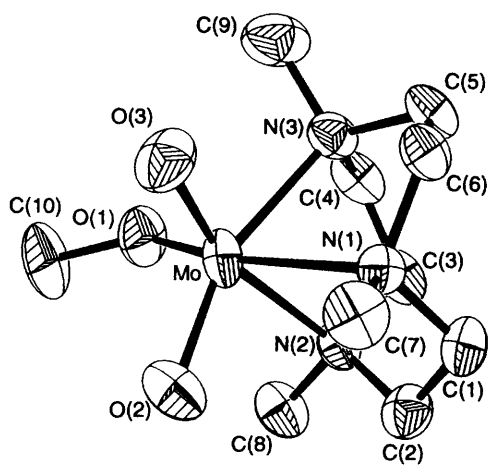

Fig. 6 Structure of the monocation in crystals of complex **6**

for **3**. The Mo–N distances in **2** and **3** are again identical within experimental error. The difference of the electronic structure of **2** (d^1) and **3** (d^2) is not reflected in these bond distances. Interestingly, the Mo–I bond lengths differ by 0.10 Å; those in **3** are longer. This is taken as an indication that the Mo^{IV}–I bond in **3** is weaker because the π-donor iodide is bound to the electron-richer metal centre Mo^{IV} as compared to that in **2**. The Mo–I bond lengths in **2** and **3** are comparable to those in $[NEt_4][MoOI_4(H_2O)]$ at 2.76 Å.[27]

Figs. 5 and 6 display the structures of the monocations in crystals of complexes **5** and **6**, respectively. Both contain a five-co-ordinate MoL(O)(OMe) fragment but the oxidation states of the central molybdenum ion are +V in **5** and +VI in **6** and the sixth co-ordination site is occupied by a MeO^- ion in **5** and a second terminal oxo group in **6**. Both the oxo and to a lesser degree the methoxo groups are good π-donor ligands forming double bonds between the oxygen donor and the molybdenum ions. Octahedral compounds with more than one multiply bonded oxygen ligand adopt a *cis* geometry which maximizes π bonding and minimizes the population of π-antibonding orbitals.[26] Consequently all O–Mo–O bond angles in **5** and **6** are > 90°. The Mo–O–C bond angle has repeatedly served as an indicator of the extent of Mo=O double-bond formation according to the three resonance structures shown. Both the relatively

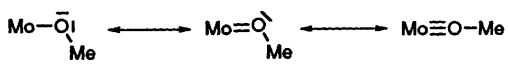

short Mo–OMe bond distances (1.92 Å in **5**, and 1.90 Å in **6**) and the Mo–O–C bond angles are in accord with a description of the bonding as shown in the second resonance structure.

When a solid sample of $[Mo_2L_2O_3(\mu\text{-}O)I][BPh_4]_2$ **9** was slowly recrystallized from MeCN solution in an open vessel at ambient temperature nice large, red-brown prisms suitable for a crystal structure determination were obtained. This material proved to be a mixed crystal containing both **9** and its oxidized and hydrolysed form $[Mo^{VI}{}_2L_2O_4(\mu\text{-}O)][BPh_4]_2$ **10** as is readily seen in the infrared spectrum of a *single crystal* of this material in the Mo=O stretch region between 800 and 1000 cm^{-1} (Fig. 7). Bands at 942 and 917 cm^{-1} are due to the *cis*-dioxomolybdenum(VI) moiety in **10** whereas a band at 964 cm^{-1} is assigned to the monooxomolybdenum(V) unit in **9**; those at 931 and 905 cm^{-1} are due to the *cis*-dioxomolybdenum(VI) fragment in **9** (Table 1).

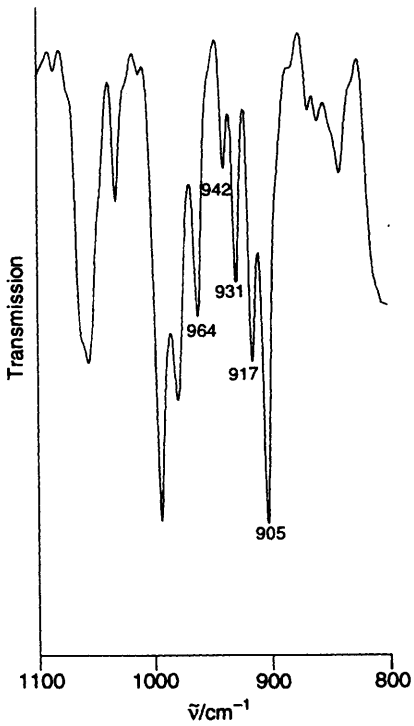

Fig. 7 Infrared spectrum (KBr disc) in the Mo=O stretch region of a single crystal of complex **9**. The bands due to Mo=O stretching modes are designated by their wavenumbers. All other bands are due to the $[BPh_4]^-$ anions and the co-ordinated amine L

The crystal-structure determination of such a single crystal allows us to establish unambiguously the presence of the two different dications of **9** and **10** in the ratio 20:80. This was achieved as follows. Complex **9** crystallizes in the monoclinic space group $P2_1/n$. The atoms of the one crystallographically independent $[BPh_4]^-$ anion and of one MoL(O) fragment were readily located by conventional Patterson and Fourier difference syntheses. The bridging oxygen atom of the Mo(1)–O–Mo(1a) unit was located on a crystallographic centre of symmetry. Thus the dinuclear cation possesses apparent crystallographic C_i symmetry. A Fourier difference map revealed at this stage two residual electron-density peaks at 2.47 and 1.65 Å from the molybdenum ion. The latter was included in the refinement as an oxygen atom with occupancy 1.0 but the anisotropic thermal parameters were physically unrealistic. When the occupancy factor of O(2) was treated as a variable (0.80) the anisotropic thermal parameters became reasonable. When the second electron-density peak was treated in the same fashion as an iodine atom (for chemical reasons) an occupancy factor of 0.20 was obtained. It is now immediately apparent that the asymmetric dication of **9** is disordered in the investigated crystal since the crystallographic site symmetry C_i is not compatible with its geometry. Fig. 8 (top) shows the structure of the symmetric dication of **10** and Fig. 8 (bottom) that of one asymmetric dication of **9**. The bond distances and angles of the symmetric dication agree remarkably with those reported for $[Mo^{VI}{}_2L_2O_4(\mu\text{-}O)][Br_3]_2$[5] but it is of course not possible to give reliable values for the disordered 'impurity' in the present structure determination. We therefore refrain from tabulating these details; they are available from the Cambridge Crystallographic Data Centre. One possible exception is the Mo^V–I bond distance of 2.469(6) Å which is shorter than the corresponding distance in **2** its mononuclear analogue. This effect has also been observed for the corresponding pair $[Mo^V{}_2\{HB(pz)_3\}_2O_2(\mu\text{-}O)Cl_2]$[19] and $[Mo\{HB(dmpz)_3\}_2O_3(\mu\text{-}O)Cl]$[20] (dmpz = 3,5-dimethylpyrazolyl) where the Mo–Cl bond distance decreases from 2.35 Å in the former to 2.14 Å in the latter. The oxo *bridge* in **9** is a poorer π donator than a

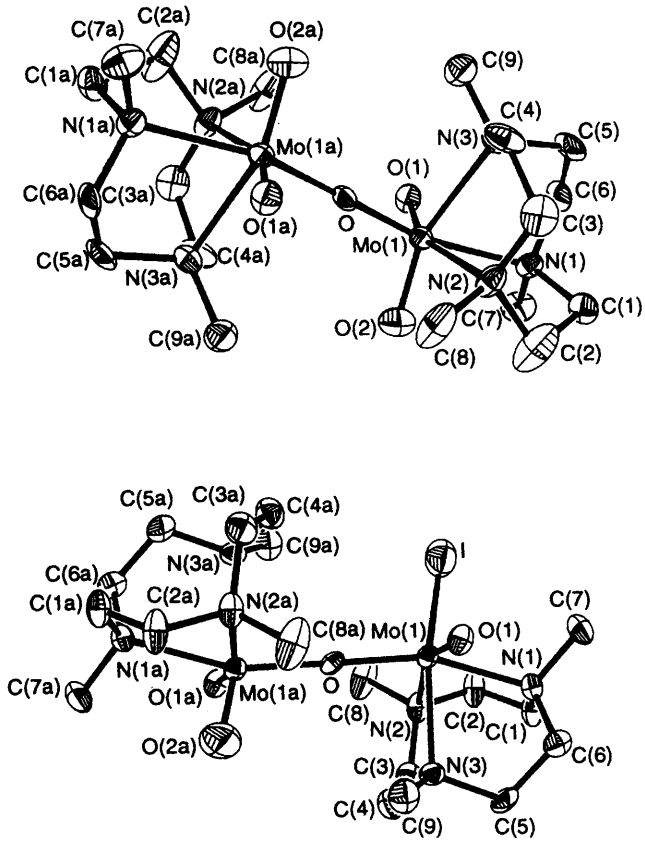

Fig. 8 Structure of the symmetric dication **10** (top) and of the asymmetric dication **9** (bottom) in a red-brown crystal of complex **9**

second iodo ligand and, consequently, the iodo ligand in **9** is allowed to act as a stronger π donor.

Electrochemistry.—Cyclic voltammograms of the complexes (≈10^{-4} mol dm^{-3}) were recorded at 20 °C in MeCN solutions containing 0.10 mol dm^{-3} tetra-*n*-butylammonium hexafluorophosphate as supporting electrolyte. The ferrocenium–ferrocene couple was used as internal reference. A glassy carbon working electrode, a platinum-wire auxiliary electrode and a Ag–AgCl (saturated LiCl in ethanol) reference electrode were used throughout. Under our experimental conditions the redox potential of ferrocene–ferrocenium was +0.54 V *vs.* Ag–AgCl (+0.40 V *vs.* normal hydrogen electrode, NHE). The results are summarized in Table 4.

The cyclic voltammogram of $[Mo^{III}LI_3]$ **1** exhibits a reversible one-electron oxidation wave at +0.525 V [equation (2)]. The complex $[MoL(O)I_2]PF_6$ **2** was found to be reversibly reduced under the same conditions at −0.25 V [equation (3)],

$$[Mo^{III}LI_3] \rightleftharpoons [Mo^{IV}LI_3]^+ + e^- \quad (2)$$

$$[Mo^{V}L(O)I_2]^+ + e^- \rightleftharpoons [Mo^{IV}L(O)I_2] \quad (3)$$

yielding complex **3**. As expected, the cyclic voltammogram of **3** is identical with that of **2**. Substitution of an iodo ligand in **2** by a methoxo group as in **4** leads to a pronounced cathodic shift of the Mo^V–Mo^{IV} redox potential of ≈0.7 V ($E_{\frac{1}{2}}$ = −0.96 V [equation (4)]. Substitution of the remaining iodo ligand in **4** by

$$[Mo^{V}L(O)(OMe)I]^+ + e^- \rightleftharpoons [Mo^{IV}L(O)(OMe)I] \quad (4)$$

a second MeO^- group in **5** results in a further cathodic shift of the Mo^V–Mo^{IV} redox potential by ≈0.7 V ($E_{\frac{1}{2}}$ for **5**: −1.68 V). Interestingly, this stabilization of the +V oxidation state in **5** brings about the accessibility of the +VI oxidation state. Thus

Table 4 Electrochemical data for the complexes[a]

Complex	$E_{\frac{1}{2}}$/V *vs.* ferrocenium–ferrocene
1	+0.525 (r)
2	−0.25 (r)
3	*b*
4	−0.96 (r)
5	+0.22 (r), −1.68 (r)
6	*c*
8	−0.34 (r), +0.51 (i), −1.45 (i)
9	*d*

[a] Cyclic voltammetry: solvent MeCN; 0.10 mol dm^{-3} $[NBu^n_4]PF_6$ supporting electrolyte; [complex] ≈ 10^{-4} mol dm^{-3}; glassy carbon electrode; Ag–AgCl(saturated LiCl–EtOH) reference electrode; ferrocenium–ferrocene couple as internal reference; scan rate 20–200 mV s^{-1}; potential range investigated +2.0 to −2.0 V *vs.* Ag–AgCl. [b] Same behaviour as that of complex **2**. [c] No redox behaviour observed. [d] Same behaviour as that of complex **8**. r = Reversible, i = irreversible (peak potential is given).

in the cyclic voltammogram of **5** a second reversible one-electron oxidation wave is detected at +0.22 V. This is a rare case of a stable monooxomolybdenum(VI) moiety in a non-aqueous solvent, equation (5). Enemark and co-workers[8a,9]

$$[Mo^{IV}L(O)(OMe)_2] \underset{+e^-}{\overset{-e^-}{\rightleftharpoons}} [Mo^{V}L(O)(OMe)_2]^+ \underset{+e^-}{\overset{-e^-}{\rightleftharpoons}} [Mo^{VI}L(O)(OMe)_2]^{2+} \quad (5)$$

have reported similar electrochemical behaviour for $[Mo^V\{HB(pz)_3\}O(OMe)_2]$. It has not been possible to isolate this species. From electrochemically oxidized solutions of **5** only the $[Mo^{VI}LO_2(OMe)]^+$ species **6** has been isolable which is the hydrolysis product of the putative $[Mo^{VI}L(O)(OMe)_2]^{2+}$ species.

Complex **6** is redox inactive in the potential range −2.0 to +2.0 V *vs.* Ag–AgCl indicating that the reduced form $[Mo^VLO_2(OMe)]$ containing a *cis*-dioxomolybdenum(v) core is not accessible. This observation bears relevance to the following discussion of electrochemical behaviour of the dinuclear complexes **8**–**10**.

The cyclic voltammogram of the dinuclear $Mo^{IV}Mo^{VI}$ species **8** shows a reversible one-electron oxidation wave at −0.34 V which is assigned to the oxidation of the Mo^{IV} [equation (6)].

$$[I(O)LMo^{IV}(\mu\text{-}O)Mo^{VI}LO_2]^+ \rightleftharpoons [I(O)LMo^{V}(\mu\text{-}O)Mo^{VI}LO_2]^{2+} + e^- \quad (6)$$

This redox potential is very similar to that measured for the mononuclear couple **2**–**3**. In addition, an irreversible oxidation wave is observed at +0.51 V and an irreversible reduction wave at −1.45 V. We have not investigated these processes in further detail.

The electrochemistry of $[\{MoLO_2\}_2(\mu\text{-}O)]^{2+}$ **10** has been reported previously.[5] Two reversible one-electron reduction waves at −0.77 and −1.88 V were assigned to the formation of deep blue mixed-valence Mo^VMo^{VI} and the Mo^V_2 dinuclear complexes, equation (7). This is to our knowledge the only case

$$[Mo^{VI}_2L_2O_5]^{2+} \underset{-e^-}{\overset{+e^-}{\rightleftharpoons}} [Mo^{V}Mo^{VI}L_2O_5]^{+} \underset{-e^-}{\overset{+e^-}{\rightleftharpoons}} [Mo^{V}_2L_2O_5] \quad (7)$$

where a *cis*-dioxomolybdenum(v) fragment in a complex has been observed; $[Mo^V_2L_2O_5]$ is a very strong reductant which has not been isolated.

Discussion

One of the most interesting aspects of this work is the full characterization of the isostructural pseudo-octahedral pair of oxomolybdenum species $[MoL(O)I_2]^{+/0}$ in **2** and **3**. Their electronic structure is readily understood following the molecular orbital scheme developed for this class of compounds in the literature.[8a,9,10,26] The terminal oxo group is a strong π-donor ligand which forms a metal-to-oxygen double or triple bond. If the Mo=O vector of such a compound (in idealized C_{4v} symmetry) coincides with the *z* axis of a cartesian coordinate system and the *x*,*y* axes are directed along equatorial metal-to-ligand bonds, the predominantly non-bonding b_2 orbital (d_{xy}) is the highest occupied molecular orbital (HOMO), which is either half-filled (Mo^V, d^1) or filled (Mo^{IV}, d^2), whereas the e orbitals d_{xz}, d_{yz} are antibonding (lowest unoccupied molecular orbital, LUMO) as depicted in Fig. 9(*a*). In this scheme the five non-oxo ligands are assumed to be pure σ donors which is an oversimplification for the present series of MoL(O)X(Y) complexes with X and Y being halide ions or alkoxo groups. These ligands are fairly strong π donors. Fig. 9(*b*) emphasizes the π interaction of such ligands with the d_{xy} orbital. Thus the stronger the π-donor ability of X or Y the more destabilized is the HOMO (b_2) and the energy gap between the b_2 and the antibonding e orbitals decreases, and the lowest-energy d–d transition in the electronic spectrum is expected to be shifted to lower energies with increasing π-donor ability of X and Y. This is indeed observed for the series of $[Mo^VL(O)X(Y)]^+$ complexes and $[Mo^V\{HB(pz)_3\}(O)X(Y)]$ complexes as is shown in Table 5. It follows that the π-donor ability increases in the order Cl < Br < I ≪ OMe, although, as noted above, the spectrum of complex **2** does not seem to fit into the series well. The large molar absorption coefficient of the lowest-energy transition for **2** implies that this band is not a pure (d–d) transition. It is also apparent from this compilation of data that both the neutral triamine L and the hydrotris(pyrazolyl)borate anion are pure σ donors. Substitution of one by the other does not change the character of the electronic structure of a given species.

The above bonding description also accounts nicely for the structural differences (or similarities) between the molybdenum-(v) and -(IV) species **2** and **3**. Upon reduction of **2** by one electron the b_2 orbital is filled ($S = 0$ ground state) which is non-bonding in the first approximation assuming pure σ bonding of all non-oxo ligands and, consequently, the metal-to-ligand distances are not expected to be different in both structures. On the other hand, if the iodo ligands behave as π donors the b_2 orbital will be antibonding and the Mo–I distance should increase somewhat on going from **2** to **3**. This is observed.

Enemark and co-workers[9] have shown for a large series of $[Mo\{HB(pz)_3\}(O)X(Y)]$ complexes that the redox behaviour (Mo^V–Mo^{IV} redox potential) is predominantly governed by the energy of the half-filled HOMO (b_2). Thus strong π-donor ligands X and Y destabilize the b_2 orbital and will make it more difficult to reduce the molybdenum(v) species. This is also true for the present series (Tables 4 and 5). This approach follows closely the idea of a linear correlation between orbital energies and redox potentials of an isoelectronic series of complexes and implies ligand additivity.[28]

It is noteworthy that relatively strong π-donating alkoxo ligands shift the energy of the HOMO in $[Mo^VLO(OR)_2]^+$ and $[Mo^V\{HB(pz)_3\}O(OR)_2]$ complexes to such energies that a reversible one-electron *oxidation* becomes feasible at electrochemically accessible potentials.[8,9] Despite many attempts both in our and Enemark's laboratory, isolation of such a monooxomolybdenum(VI) species containing a $Mo^{VI}L(O)$ or $Mo^{VI}\{HB(pz)_3\}O$ fragment has not yet been achieved. Part of the problem appears to be the fast and very efficient hydrolysis of an alkoxo ligand by water generating thermodynamically very stable complexes containing a *cis*-dioxomolybdenum(VI) moiety. In our chemistry $[Mo^{VI}LO_2(OMe)]^+$ **6** is the isolable species.

Table 5 Compilation of electronic spectral and electrochemical data for the molybdenum(v) complexes

Complex	$E(MoO^{3+}-MoO^{2+})^a$/V	$10^{-3}E_{max}$/cm^{-1} (ε/dm^3 mol^{-1} cm^{-1})^b
$[MoL(O)Cl_2]^+$	−0.52	15.10 (37)
$[MoL(O)Br_2]^+$	−0.40	14.84 (10)
$[MoL(O)I_2]^+$	−0.25	15.13 (1800)
$[MoL(O)I(OMe)]^+$	−0.96	*c*
$[MoL(O)(OMe)_2]^+$	−1.68	14.29 (25)
$[Mo\{HB(dmpz)_3\}(O)Cl_2]$	−0.79	14.18 (50)
$[Mo\{HB(dmpz)_3\}(O)Cl(OMe)]$	−1.38	12.90 (30)
$[Mo\{HB(dmpz)_3\}O(OMe)_2]$	−1.64	12.99 (90)

[a] Redox potential referenced to ferrocenium–ferrocene. [b] Lowest-energy d–d transition. [c] Not measured.

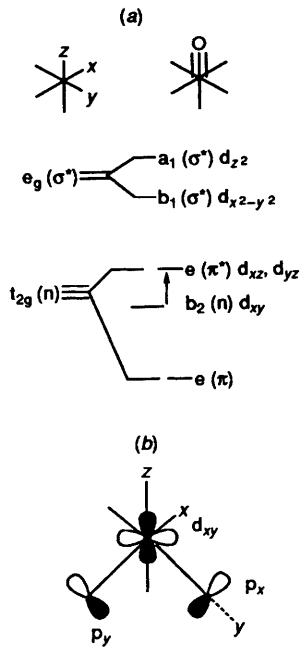

Fig. 9 (*a*) Qualitative MO scheme for pseudo-octahedral $MoOX_5$ complexes in C_{4v} symmetry. The arrow indicates the energetically lowest d–d transition ($^2B_2 \longrightarrow {}^2E$ for d^1 species). (*b*) Schematic representation of the π-bonding between two equatorial ligands X, Y and the d_{xy} orbital in complexes of the type $[MoL(O)X(Y)]^{+/0}$

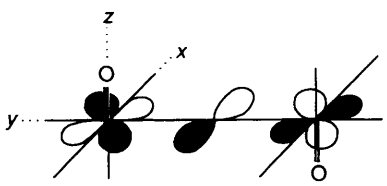

In the following section we discuss some aspects of the dinuclear complexes **7**–**9**. Complex **7**, a diamagnetic species with a $[Mo^V_2O_2(\mu\text{-}O)]^{4+}$ core, is readily obtained by Tl^I-assisted base hydrolysis of mononuclear **2**. Its diamagnetism is understood by a magnetic π-superexchange mechanism. Assuming a coordinate system where the *z* axis coincides with the short Mo=O vector of the $Mo^VL(O)$ fragment, the unpaired electron (d^1, Mo^V) resides then in a d_{xy} metal orbital which strongly overlaps with a filled p orbital of the oxo bridge yielding strong intramolecular antiferromagnetic coupling of the two d_{xy}^1 electrons. It is very interesting that further base hydrolysis of **7** yields the mixed-valence species **8** with a $[OMo^{IV}(\mu\text{-}O)Mo^{VI}O_2]^{2+}$ core. Complex **8** is diamagnetic ($S = 0$). The reaction may be described as an intramolecular disproportionation initiated by hydrolysis. Its driving force may be rationalized by using the above MO description (Fig. 9) for the mononuclear oxomolybdenum-(IV), -(V), -(VI) and the

Table 6 Elemental analyses of the complexes (calculated values in parentheses)

		Analysis (%)		
Complex	*M*	C	H	N
1 $[MoLI_3]$	647.9	16.7 (16.70)	3.3 (3.25)	6.5 (6.5)
2 $[MoL(O)I_2]PF_6$	682.0	15.9 (15.85)	2.9 (3.1)	6.3 (6.15)
3 $[MoL(O)I_2]$	537.0	19.9 (20.1)	3.8 (3.9)	7.6 (7.8)
5 $[MoL(O)(OMe)_2]PF_6$	490.3	26.8 (26.95)	5.4 (5.55)	8.5 (8.55)
6 $[MoLO_2(OMe)]PF_6$	475.2	25.2 (25.25)	5.0 (5.1)	8.7 (8.85)
7 $[Mo_2L_2O_3I_2][PF_6]_2$	1126.2	19.5 (19.2)	3.7 (3.75)	7.5 (7.45)
8 $[Mo_2L_2O_4I]BPh_4$	1044.6	48.0 (48.3)	5.8 (6.0)	8.2 (8.05)
9 $[Mo_2L_2O_4I][BPh_4]_2$	1363.8	57.9 (58.15)	6.1 (6.1)	6.1 (6.15)

-*cis*-dioxomolybdenum(VI) complexes. The HOMO of one half of the putative intermediate $[I(O)LMo^V(\mu\text{-}O)Mo^VO(OH)L]^{2+}$ is significantly destabilized by deprotonation of the terminal hydroxo ligand which is thereby transformed into a strong π donor (a terminal oxo group). Thus the energy of the HOMO of the $[O_2LMo^V(\mu\text{-}O)]^-$ unit is much more unfavourable than that in the $[I(O)LMo^V(\mu\text{-}O)]$ half of the dinuclear species. Intramolecular electron transfer from the first to the second half generates then a low-lying filled and an empty d_{xy} orbital. Fully in accord with this description is the observation of a reversible one-electron oxidation of **8** with formation of the paramagnetic mixed-valence Mo^VMo^{VI} complex **9**.

From the above discussion it immediately follows that the mixed-valence species **8** and **9** are to be described as class I complexes with localized oxidation states according to Robin and Day.[22] In contrast, the symmetric complex **10** containing a $[Mo^{VI}_2O_4(\mu\text{-}O)]^{2+}$ core with a linear Mo–O–Mo group is reversibly reduced to the Mo^VMo^{VI} mixed-valence species.[5] In this case, as in similar compounds of this type,[18] the valences are delocalized.

Experimental

Materials and Methods.—The preparations of the ligand 1,4,-7-trimethyl-1,4,7-triazacyclononane and the complex $[MoL(CO)_3]$ have been described previously.[4] All other chemicals were purchased from commercial sources and used as supplied. Infrared spectra were recorded on a Perkin Elmer 1720 X FT spectrometer as KBr discs, electronic spectra on a Perkin Elmer Lambda 9 UV/VIS/NIR spectrophotometer in the range 200–1500 nm. Temperature-dependent magnetic susceptibilities were measured in the range 80–298 K by using the Faraday method. Corrections for underlying diamagnetism of solid samples were applied by use of Pascal's constants. Cyclic

Table 7 Crystal data and data collection parameters* for the structures of complexes **2**, **3**, **5**, **6** and **9**

	2	**3**	**5**	**6**	**9**
Molecular formula	$C_9H_{21}F_6I_2MoN_3OP$	$C_9H_{21}I_2MoN_3O$	$C_{11}H_{27}F_6MoN_3O_3P$	$C_{34}H_{41}BMoN_3O_3$	$C_{66}H_{82}B_2I_{0.2}Mo_2N_6O_{4.8}$
M	682.0	537.0	490.3	646.4	1275
Crystal colour, habit	Black, bipyramidal	Violet, prismatic	Blue, prism	Faint bluish, prism	Red-brown, prism
Crystal size/mm	0.2 × 0.3 × 0.4	0.4 × 0.4 × 0.6	0.4 × 0.3 × 0.5	0.6 × 0.7 × 0.4	0.3 × 0.6 × 0.22
Space group	*Pbcm* (no. 57)	$P2_1/c$ (no. 14)	*Pnma*	$P2_1/n$	$P2_1/n$
a/Å	7.724(2)	7.724(2)	12.978(3)	10.405(5)	12.361(2)
b/Å	14.731(4)	14.263(3)	11.521(2)	21.177(6)	18.568(4)
c/Å	16.414(5)	13.865(3)	12.937(3)	15.447(4)	13.442(3)
β/°		96.70(2)		91.81(3)	90.90(3)
U/Å^3	1867.6(10)	1517.0(10)	1934.3(7)	3402(2)	3084.8(11)
Z	4	4	4	4	2
D_c/g cm^{-3}	2.42	2.35	1.68	1.26	1.38
F(000)	1284	1008	996	1348	1329
μ(Mo-Kα)/mm^{-1}	4.10	4.86	0.81	0.41	0.55
Diffractometer	Syntex R3	Syntex R3	Siemens P4	Siemens P4	Siemens P4
2θ range/°	3–60	3–60	3–55	3–55	3–50
Reflections measured	3100	4864	2538	8521	5870
Observed reflections (criterion)	1850[$I \geqslant 2.5\sigma(I)$]	2053[$I \geqslant 2.5\sigma(I)$]	1723[$I \geqslant 2.5\sigma(I)$]	5194[$I \geqslant 2.0\sigma(I)$]	3018[$I \geqslant 2.5\sigma(I)$]
Least-squares parameters	112	146	124	395	539
R	0.052	0.091	0.067	0.050	0.034
R'	0.047	0.075	0.077	0.056	0.033

* Details in common: T = 298 K; Mo-Kα radiation (λ = 0.710 73 Å), ω-scan mode; absorption correction, empirical ψ scans of seven reflections.

voltammograms were recorded on PAR equipment consisting of a model 173/179 potentiostat/galvanostat and a model 175 universal programmer. The ESR spectra were recorded on a Bruker ER 200 spectrometer.

Preparation of Complexes.—Table 6 summarizes elemental analyses of complexes.

$[Mo^{III}LI_3]$ **1**. To a suspension of $[MoL(CO)_3]$ (5.2 g, 14 mmol) in concentrated HI (100 cm^3) was added elemental iodine (1.0 g). The reaction mixture was heated to reflux in the presence of air for 5 h. To the orange-brown solution was added water (50 cm^3) and heating was continued for 2 h. An orange microcrystalline solid precipitated which was filtered off and dried *in vacuo*. Recrystallization from a saturated acetonitrile solution afforded crystals suitable for single-crystal X-ray crystallography (yield: 5.9 g; 64%).

$[Mo^{V}L(O)I_2]PF_6$ **2**. A suspension of complex **1** in ≈7 mol dm^{-3} nitric acid (20 cm^3) was stirred at room temperature for 1 h in the presence of air whereupon a colour change from orange to dark green occurred and elemental iodine precipitated. After removal of the iodine by filtration a saturated aqueous solution of $NaPF_6$ (10 cm^3) was added. A green precipitate formed which was filtered off and dried *in vacuo* over P_4O_{10}. Single crystals for X-ray crystallography were grown from acetonitrile–mesitylene (1:1) (yield: 0.38 g; 80%).

$[Mo^{IV}L(O)I_2]$ **3**. To a solution of complex **2** (0.4 g, 0.6 mmol) in deoxygenated MeCN (50 cm^3) was added deoxygenated triethylamine (1 cm^3). The resulting dark green solution was allowed to stand at ambient temperature under an argon atmosphere for 1 h during which time pink crystals of **3** precipitated. These were filtered off and dried *in vacuo* over P_4O_{10}. Single crystals of **3** were slowly grown from nitromethane–mesitylene (1:1) containing a few drops of NEt_3 (yield: 0.27 g; 84%).

$[Mo^{V}L(O)(OMe)I]PF_6$ **4**. To a solution of complex **2** (0.68 g, 1.0 mmol) in deoxygenated methanol (50 cm^3) was added Tl(OMe) (0.25 g, 1.0 mmol). The dark green reaction mixture was heated to reflux for 5 h under an argon atmosphere. Yellow TlI precipitated and was filtered off. After reduction of the reaction volume to 10 cm^3 by evaporation, a dark green precipitate formed and was filtered off. The material is not quite pure; it contains small amounts of unreacted **2** and $[Mo^{V}L(O)(OMe)_2]PF_6$ which could not be removed by recrystallization. Further purification of **4** was not attempted.

$[Mo^{V}L(O)(OMe)_2]PF_6$ **5**. To a solution of complex **2** (0.68 g, 1.0 mmol) in deoxygenated methanol (50 cm^3) was added Tl(OMe) (0.5 g, 2.0 mmol). The suspension was heated to reflux for 5 h under an argon atmosphere. Yellow TlI precipitated and the colour of the solution changed to deep blue. After removal of TlI by filtration and reduction of the volume to ≈10 cm^3 by evaporation under reduced pressure a deep blue crystalline precipitate formed and was filtered off. Recrystallization from acetonitrile–toluene (1:1) under argon yielded single crystals suitable for X-ray crystallography (yield: 0.31 g; 63%).

$[Mo^{VI}LO_2(OMe)]PF_6$ **6**. To a solution of complex **5** (0.5 g, 1.0 mmol) in methanol (30 cm^3) was added 30% H_2O_2 (10 cm^3). The solution was heated to reflux until a clear colourless solution was obtained. Addition of $NaPF_6$ (0.3 g) and reduction of the reaction volume to 10 cm^3 by evaporation under reduced pressure initiated the precipitation of colourless crystals which were filtered off. Single crystals of $[Mo^{VI}LO_2(OMe)]BPh_4$ were grown by slow air oxidation of **5** in MeCN and $NaBPh_4$ (yield: 0.3 g; 61%).

$[Mo^{V}_2L_2O_2(\mu\text{-}O)I_2][PF_6]_2$ **7**. A suspension of complex **2** (0.68 g, 1.0 mmol) and Tl(acac) (0.3 g, 1.0 mmol) in deoxygenated MeCN (25 cm^3) containing ≈2% water was heated to reflux for 3 h under argon. A colour change from green to red-brown was observed. After removal of TlI by filtration the reaction volume was reduced to 10 cm^3 by evaporation under reduced pressure. Addition of $CHCl_3$ (50 cm^3) initiated the precipitation of red-brown microcrystals which were filtered off (yield: 0.30 g; 52%).

$[Mo_2L_2O_3(\mu\text{-}O)I]BPh_4$ **8**. To a solution of complex **7** (0.56 g, 0.5 mmol) in acetone (20 cm^3) was added a solution of 0.5 mol dm^{-3} NaOH (5 cm^3). After stirring for 5 min at ambient temperature the colour had changed from brown-red to deep blue. Addition of a saturated aqueous solution of $NaBPh_4$ (2 cm^3) initiated the precipitation of a microcrystalline deep blue solid which was filtered off and dried *in vacuo* over P_4O_{10}. Recrystallization was from nitromethane by slow diffusion of diethyl ether (yield: 0.35 g; 67%).

$[Mo_2L_2O_3(\mu\text{-}O)I][BPh_4]_2$ **9**. To a solution of complex **8** (0.1 g; 0.10 mmol) in MeCN (20 cm^3) was added dropwise a solution of ferrocenium hexafluorophosphate (0.16 g, 0.15 mmol) in MeCN (5 cm^3). The colour changed from deep blue to orange. Excess of the oxidant causes a colour change to blue and must be avoided. Addition of a saturated MeCN solution

Table 8 Atomic coordinates ($\times 10^4$)

Atom	*x*	*y*	*z*	Atom	*x*	*y*	*z*
Compound 2							
I(1)	1 503(1)	457(1)	1 324(1)	C(3)	−1 120(12)	−1 559(6)	4 082(5)
Mo	−103(1)	−500(1)	2 500	C(4)	−2 063(17)	1 505(7)	2 500
O	1 048(10)	−1 456(5)	2 500	C(5)	−2 913(18)	−1 869(7)	2 910(6)
N(1)	−2 509(11)	496(6)	2 500	P	6 388(4)	2 500	0
N(2)	−2 032(9)	−1 123(5)	3 361(4)	F(11)	6 399(10)	2 119(6)	−880(4)
C(1)	−3 566(17)	322(7)	3 213(9)	F(12)	4 972(11)	1 831(6)	264(5)
C(2)	−3 328(15)	−461(9)	3 673(6)	F(13)	7 848(9)	1 849(5)	286(4)
Compound 3							
Mo	2 911(2)	32(1)	7 704(1)	C(2)	429(36)	−1 295(18)	8 709(18)
I(1)	2 108(2)	1 484(1)	8 924(1)	C(3)	3 055(36)	−1 964(16)	8 303(19)
I(2)	2 920(2)	1 359(1)	6 222(1)	C(4)	3 011(39)	−2 042(20)	7 302(16)
O	5 046(16)	−73(9)	8 062(10)	C(5)	1 324(34)	−1 280(21)	6 104(18)
N(1)	−102(24)	−264(12)	7 253(11)	C(6)	−222(38)	−935(18)	6 404(18)
N(2)	2 303(21)	−1 143(11)	8 698(11)	C(7)	−1 266(27)	530(13)	7 011(15)
N(3)	2 903(22)	−1 200(11)	6 713(12)	C(8)	3 066(30)	−1 009(14)	9 722(14)
C(1)	−766(32)	−793(21)	8 091(18)	C(9)	4 355(31)	−1 201(14)	6 115(16)
Compound 5							
Mo	8 578(1)	2 500	1 387(1)	C(4)	8 913(8)	4 791(10)	2 643(10)
O(1)	7 703(5)	2 500	2 347(6)	C(5)	9 894(8)	3 122(9)	3 283(6)
O(2)	8 207(4)	3 748(4)	499(4)	C(6)	7 398(6)	3 952(8)	−210(7)
N(1)	10 201(5)	2 500	577(5)	P	6 398(3)	7 500	1 316(2)
N(2)	9 543(4)	3 746(5)	2 322(4)	F(1)	7 026(9)	7 500	303(8)
C(1)	10 754(6)	3 554(8)	863(7)	F(2)	5 742(12)	7 500	2 258(8)
C(2)	10 438(7)	4 189(7)	1 731(7)	F(3)	5 691(8)	6 647(9)	766(7)
C(3)	10 014(9)	2 500	−601(8)	F(4)	6 950(12)	6 565(12)	1 783(10)
Compound 6							
Mo	2 368(1)	690(1)	6 371(3)	C(14)	9 789(6)	2 454(3)	4 481(3)
N(1)	2 663(3)	598(2)	7 821(2)	C(15)	8 550(6)	2 324(3)	4 651(3)
N(2)	3 102(4)	1 679(2)	6 788(2)	C(16)	7 885(5)	2 680(2)	5 260(3)
N(3)	601(4)	1 195(2)	6 913(2)	C(17)	8 369(4)	3 249(2)	7 368(3)
O(1)	1 831(4)	1 031(2)	5 288(2)	C(18)	9 508(4)	3 465(2)	7 781(3)
O(2)	4 017(4)	496(2)	6 194(3)	C(19)	10 076(5)	3 158(3)	8 492(3)
O(3)	1 540(4)	−48(2)	6 386(2)	C(20)	9 533(6)	2 633(3)	8 830(3)
C(1)	3 362(5)	1 155(2)	8 213(3)	C(21)	8 427(5)	2 399(2)	8 438(3)
C(2)	3 997(5)	1 547(2)	7 534(3)	C(22)	7 868(5)	2 698(2)	7 731(3)
C(3)	2 048(5)	2 110(2)	7 047(3)	C(23)	6 199(4)	3 562(2)	6 407(3)
C(4)	759(5)	1 877(2)	6 721(3)	C(24)	5 547(5)	3 658(2)	5 614(3)
C(5)	504(5)	1 071(3)	7 868(3)	C(25)	4 245(5)	3 731(2)	5 524(3)
C(6)	1 354(5)	527(2)	8 163(3)	C(26)	3 493(5)	3 708(2)	6 233(4)
C(7)	3 420(5)	14(2)	8 026(3)	C(27)	4 081(5)	3 624(2)	7 030(4)
C(8)	3 827(5)	1 973(2)	6 076(3)	C(28)	5 415(4)	3 547(2)	7 117(3)
C(9)	−590(6)	981(3)	6 466(4)	C(29)	8 095(4)	4 332(2)	6 450(3)
C(10)	2 137(9)	915(4)	4 427(4)	C(30)	8 352(5)	4 661(2)	5 691(3)
B	7 780(5)	3 576(2)	6 481(3)	C(31)	8 473(5)	5 313(2)	5 660(3)
C(11)	8 459(4)	3 181(2)	5 705(3)	C(32)	8 344(5)	5 664(3)	6 392(4)
C(12)	9 743(5)	3 290(2)	5 503(3)	C(33)	8 093(5)	5 367(2)	7 161(4)
C(13)	10 391(5)	2 935(3)	4 908(3)	C(34)	7 964(4)	4 718(2)	7 175(3)
Compound 9							
Mo(1)	147(1)	6 009(1)	5 180(1)	C(13)	1 709(5)	8 881(3)	−2 302(4)
O	0	5 000	5 000	C(14)	777(5)	8 996(3)	−1 776(4)
O(1)	−1 132(3)	6 291(2)	5 491(2)	C(15)	544(4)	8 569(3)	−960(4)
N(1)	750(3)	7 071(2)	5 803(3)	C(16)	3 479(5)	5 930(3)	1 229(5)
N(2)	2 050(3)	5 871(2)	5 325(3)	C(17)	3 162(5)	6 457(3)	1 871(5)
O(2)	344(5)	6 307(3)	4 038(3)	C(18)	2 365(4)	6 950(3)	1 592(4)
I	427(5)	6 463(3)	3 476(4)	C(19)	1 846(4)	6 939(3)	666(4)
N(3)	540(3)	5 765(2)	6 861(3)	C(20)	2 199(5)	6 391(3)	37(4)
C(1)	1 962(5)	7 156(3)	5 786(5)	C(21)	2 996(5)	5 902(3)	300(5)
C(2)	2 465(6)	6 606(3)	5 127(6)	C(22)	559(4)	8 029(3)	1 243(3)
C(3)	2 420(5)	5 607(4)	6 333(5)	C(23)	−1 151(5)	1 350(3)	8 554(4)
C(4)	1 504(5)	5 286(3)	6 896(5)	C(24)	−965(5)	900(3)	7 765(4)
C(5)	755(5)	6 456(3)	7 428(4)	C(25)	−141(5)	1 058(4)	7 122(4)
C(6)	355(5)	7 099(3)	6 852(4)	C(26)	462(5)	1 651(4)	7 280(4)
C(7)	240(7)	7 680(3)	5 235(6)	C(27)	264(4)	2 097(3)	8 078(4)
C(8)	2 441(6)	5 377(4)	4 545(7)	C(28)	−202(4)	6 979(2)	3(3)
C(9)	−399(6)	5 381(4)	7 309(5)	C(29)	−430(5)	6 347(3)	518(4)
B	858(4)	7 487(3)	312(4)	C(30)	−1 289(5)	5 897(3)	286(5)
C(10)	1 213(4)	8 004(3)	−634(3)	C(31)	3 017(5)	8 933(4)	4 511(5)
C(11)	2 169(4)	7 925(3)	−1 175(4)	C(32)	−1 813(5)	6 678(3)	−1 015(5)
C(12)	2 414(5)	8 354(3)	−1 980(4)	C(33)	−934(4)	7 123(3)	−779(4)

of $NaBPh_4$ (5 cm^3) initiated the precipitation of orange-red microcrystals which were filtered off (yield: 0.10 g; 76%).

Crystal Structure Analyses.—Table 7 summarizes the relevant data for the crystal structure determinations. Final atom coordinates are given in Table 8 for structures of **2**, **3**, **5**, **6** and **9**. Intensity data were corrected for Lorentz polarization and absorption effects (ψ scans) in the usual manner. The structures were solved by conventional Patterson and Fourier difference methods by using the SHELXTL-PLUS (PC version) program package.[29] The function minimized during full-matrix least-squares refinement was $\Sigma w(|F_o| - |F_c|)^2$ where $w^{-1} = \sigma^2(F)$. Neutral atom scattering factors and anomalous dispersion corrections for non-hydrogen atoms were taken from ref. 30. The positions of the hydrogen atoms were calculated and included with fixed isotropic thermal parameters. All other atoms were refined with anisotropic thermal parameters. Some special features of the crystal structure determination are: **2**, the positions of hydrogen atoms were not calculated and were not included in the final refinement cycle; **3**, the available crystals were of low X-ray quality but the structure determination establishes unambiguously the chemical composition and atom connectivity.

Additional material available from the Cambridge Crystallographic Data Centre comprises H-atom coordinates, thermal parameters and remaining bond lengths and angles.

Acknowledgements

We thank Fonds der Chemischen Industrie for financial support and Dr. E. Bill (Medizinische Universtät Lübeck) for recording the ESR spectra.

References

1 C. D. Garner and J. M. Charnock, in *Comprehensive Coordination Chemistry*, eds. G. Wilkinson, R. D. Gillard and J. A. McCleverty, Pergamon, Oxford, 1987, vol. 3, p. 1329.
2 (*a*) R. H. Holm, *Coord. Chem. Rev.*, 1990, **100**, 183; (*b*) R. H. Holm and J. M. Berg, *Acc. Chem. Res.*, 1986, **19**, 363; (*c*) R. H. Holm, *Chem. Rev.*, 1987, **87**, 1401.
3 R. Bhula, P. Osvath and D. C. Weatherburn, *Coord. Chem. Rev.*, 1988, **91**, 89; P. Chaudhuri and K. Wieghardt, *Prog. Inorg. Chem.*, 1987, **35**, 329.
4 G. Backes-Dahmann, W. Herrmann, K. Wieghardt and J. Weiss, *Inorg. Chem.*, 1985, **24**, 485.
5 K. Wieghardt, G. Backes-Dahmann, W. Herrmann and J. Weiss, *Angew. Chem.*, 1984, **96**, 890; *Angew. Chem., Int. Ed. Engl.*, 1984, **23**, 899.
6 P. S. Roy and K. Wieghardt, *Inorg. Chem.*, 1987, **26**, 1885; K. Wieghardt, M. Hahn, W. Swiridoff and J. Weiss, *Inorg. Chem.*, 1984, **23**, 94; W. Herrmann and K. Wieghardt, *Polyhedron*, 1986, **5**, 513; G. Haselhorst, S. Stötzel, A. Strassburger, W. Walz, K. Wieghardt and B. Nuber, *J. Chem. Soc., Dalton Trans.*, 1993, 83.
7 U. Bossek, P. Knopp, C. Habenicht, K. Wieghardt, B. Nuber and J. Weiss, *J. Chem. Soc., Dalton Trans.*, 1991, 3165.
8 (*a*) W. E. Cleland, jun., K. M. Barnhart, K. Yamanouchi, D. Collison, F. E. Mabbs, R. B. Ortega and J. H. Enemark, *Inorg. Chem.*, 1987, **26**, 1017; (*b*) S. Trofimenko, *Inorg. Chem.*, 1971, **10**, 504; (*c*) M. Minelli, K. Yamanouchi, J. H. Enemark, P. Subramanian, B. B. Kaul and J. T. Spence, *Inorg. Chem.*, 1984, **23**, 2554.
9 C. S. J. Chang, D. Collison, F. E. Mabbs and J. H. Enemark, *Inorg. Chem.*, 1990, **29**, 2261.
10 C. S. J. Chang and J. H. Enemark, *Inorg. Chem.*, 1991, **30**, 683.
11 M. Millar, S. Lincoln and S. A. Koch, *J. Am. Chem. Soc.*, 1982, **104**, 288.
12 C. S. J. Chang, A. Rai-Chaudhuri, D. L. Lichtenberger and J. H. Enemark, *Polyhedron*, 1990, **9**, 1965.
13 S. A. Roberts, C. G. Young, C. A. Kipke, W. E. Cleland, jun., K. Yamanouchi, M. D. Carducci and J. H. Enemark, *Inorg. Chem.*, 1990, **29**, 3650.
14 S. Wolowiec and J. K. Kochi, *Inorg. Chem.*, 1991, **30**, 1215.
15 S. E. Lincoln and T. M. Loehr, *Inorg. Chem.*, 1990, **29**, 1907.
16 C. A. Kipke, W. E. Cleland, jun., S. A. Roberts and J. H. Enemark, *Acta Crystallogr., Sect. C*, 1989, **45**, 870; S. A. Roberts, R. B. Ortega, L. M. Zolg, W. E. Cleland, jun. and J. H. Enemark, *Acta Crystallogr., Sect. C*, 1987, **43**, 51; C. J. S. Chang, T. J. Pecci, M. D. Carducci and J. H. Enemark, *Acta Crystallogr., Sect. C*, 1992, **48**, 1096.
17 N. E. Heimer and W. E. Cleland, jun., *Acta Crystallogr., Sect. C*, 1991, **47**, 56.
18 M. Chaudhury, *J. Chem. Soc., Dalton Trans.*, 1983, 857.
19 S. Lincoln and S. A. Koch, *Inorg. Chem.*, 1986, **25**, 1594.
20 A. A. Eagle, M. F. Mackay and C. G. Young, *Inorg. Chem.*, 1991, **30**, 1425.
21 C. G. Young, R. W. Gable and M. F. Mackay, *Inorg. Chem.*, 1990, **29**, 1777.
22 M. B. Robin and P. Day, *Adv. Inorg. Chem. Radiochem.*, 1967, **10**, 357.
23 A. K. Mohammed and A. W. Maverick, *Inorg. Chem.*, 1992, **31**, 4441.
24 H. K. Saha and A. K. Banerjee, *J. Inorg. Nucl. Chem.*, 1972, **34**, 697.
25 G. P. Haight, *J. Inorg. Nucl. Chem.*, 1962, **24**, 663, 670.
26 See W. A. Nugent and J. M. Mayer, in *Metal–Ligand Multiple Bonds*, Wiley, New York, 1988, pp. 33, 34.
27 A. Bino and F. A. Cotton, *Inorg. Chem.*, 1979, **18**, 2710.
28 See, for example, B. E. Bursten, *J. Am. Chem. Soc.*, 1982, **104**, 1299.
29 G. M. Sheldrick, SHELXTL-PLUS, Universität Göttingen, 1990.
30 *International Tables for X-Ray Crystallography*, Kynoch Press, Birmingham, 1974, vol. 4, pp. 99, 149.

Received 18*th January* 1993; *Paper* 3/00272A